

# *Caenorhabditis elegans* utilizes dauer pheromone biosynthesis to dispose of toxic peroxisomal fatty acids for cellular homeostasis

Hyo-e-Jin JOO\*, Yong-Hyeon YIM†, Pan-Young JEONG\*<sup>1</sup>, You-Xun JIN†, Jeong-Eui LEE\*, Heekyeong KIM\*<sup>2</sup>, Seul-Ki JEONG\*, David J. CHITWOOD‡ and Young-Ki PAIK\*<sup>3</sup>

\*Department of Biochemistry, College of Life Sciences and Biotechnology, Yonsei Proteome Research Center, Yonsei University, Seoul 120-749, Republic of Korea,

†Korea Research Institute of Standards and Science, Daejeon 305-340, Republic of Korea, and ‡Nematology Laboratory, USDA, ARS, Beltsville, MD 20705, U.S.A.

*Caenorhabditis elegans* excretes a dauer pheromone or daumone composed of ascarylose and a fatty acid side chain, the perception of which enables worms to enter the dauer state for long-term survival in an adverse environment. During the course of elucidation of the daumone biosynthetic pathway in which DHS-28 and DAF-22 are involved in peroxisomal  $\beta$ -oxidation of VLCFAs (very long-chain fatty acids), we sought to investigate the physiological consequences of a deficiency in daumone biosynthesis in *C. elegans*. Our results revealed that two mutants, *dhs-28(tm2581)* and *daf-22(ok693)*, lacked daumones and thus were dauer defective; this coincided with massive accumulation of fatty acyl-CoAs (up to 100-fold) inside worm bodies compared with levels in wild-type N2 worms. Furthermore, the deficiency

in daumone biosynthesis and the massive accumulation of fatty acids and their acyl-CoAs caused severe developmental defects with reduced life spans (up to 30%), suggesting that daumone biosynthesis is an essential part of *C. elegans* homeostasis, affecting survival and maintenance of optimal physiological conditions by metabolizing some of the toxic non-permissible peroxisomal VLCFAs from the worm body in the form of readily excretable daumones.

**Key words:** ascarioside, *Caenorhabditis elegans*, daumone, fatty acid, dauer larvae, nematode, peroxisomal  $\beta$ -oxidation, pheromone.

## INTRODUCTION

*Caenorhabditis elegans* excretes a dauer pheromone or daumone (Figure 1A), the perception of which allows worms to gauge food depletion or a high worm population density; the increased daumone concentration signals worms to enter the dauer state for long-term survival [1–3]. In this nonfeeding condition, worms can survive for several months in adverse environments and are capable of re-entering their life cycle when conditions are favourable for growth [1,4–6]. The sensory response to daumones is mediated by amphidial neurons [7] via a process in which the G-protein GPA-3 serves a gating function [8]. The dauer entry pathway appears compartmentalized in time and correlated with metabolic flux [9].

After the pioneering work on the existence of a dauer-inducing pheromone by the Riddle group in 1982 [1], more than two decades passed before the major breakthrough in its chemical identification and biological characterization (Figure 1A) [2]. Furthermore, several daumone analogues with different dauer-inducing activities and relative concentrations [e.g., daumone 2 (ascarioside 1, ascarioside C6 or Ascr#1) and daumone 3 (ascarioside 2, ascarioside C9 or Ascr#3), Figure 1A] were recently reported [10]. Besides dauer-inducing activity as exerted by daumones 1–3, which are the major targets of the present study, daumone 4 (Ascr#4, Figure 1A) functions as a mating signal synergistically with daumones 2 and 3 [11], whereas daumone 5 (termed ascarioside C3, Figure 1A) may act as a potent component in dauer-inducing activity [12]. Because various names have been used in the literature, here we

propose and use a unified nomenclature for dauer pheromones throughout this paper (Figure 1A). For example, daumone 1 has been referred to as ascarioside 3 [10] and ascr#1 [11].

Structurally, daumones are ascariosides, composed of a glycone moiety (the 3,6-dideoxy sugar ascarylose) and an aglycone [generally a  $\leq C_9$ -SCFA (short-chain fatty acid)] (Figure 1A). Ascariosides with long ( $C_{22-37}$ ) fatty acid aglycones occur in the egg shell and female reproductive tract of parasitic nematodes such as *Ascaris* and *Parascaris equorum* (Figure 1A) [13–17]. Within a cell, ascarylose is known to exist in a CDP-esterified form (CDP-ascarylose) and is predicted to be synthesized *de novo* from glucose-1-phosphate in *Ascaris lumbricoides* ovaries and *Yersinia pseudotuberculosis* [18–21]. Although ascarylose biosynthesis genes occur in bacteria [20,21], it is not known if *C. elegans* biosynthesizes ascarylose *de novo* or imports it from its *Escherichia coli* laboratory diet.

Considering the nature of the SCFA aglycone structure, unlike mitochondrial  $\beta$ -oxidation which completely oxidizes various short chain fatty acids ( $\leq C_9$ ) for energy production, peroxisomal  $\beta$ -oxidation processes long chain fatty acids ( $C_{15}-C_{20}$ ) or VLCFAs (very-long chain fatty acids,  $> C_{20}$ ) including straight and methyl branched chains to produce SCFAs, components of daumone (Figure 1B). It was therefore reasonable to hypothesize that peroxisomal  $\beta$ -oxidation would be involved in daumone biosynthesis. Recently, it was reported that part of the daumone biosynthesis pathway occurs in the peroxisome, wherein two enzymes, DHS-28 and DAF-22 [22], actively participate [23]. In addition to chain-shortening processes,

Abbreviations used: ACOT, acyl-CoA thioesterase; CACT, carnitine acylcarnitine translocase; D-BP, D-bifunctional protein; ESI, electrospray ionization; GFP, green fluorescent protein; LC, liquid chromatography; MLS, mean lifespan; MS/MS, tandem MS; NGM, nematode growth medium; qRT-PCR, quantitative reverse transcription-PCR; RNAi, RNA interference; SCFA, short-chain fatty acid; SCPx, sterol carrier protein x; SRM, selected reaction monitoring; UGT, UDP-glucuronyltransferase; VLCFA, very-long-chain fatty acid.

<sup>1</sup> Present address: Department of Molecular, Cellular and Developmental Biology, University of California Santa Barbara, Santa Barbara, CA 93106, U.S.A.

<sup>2</sup> Present address: Graduate Program in Biomaterials, Science and Engineering, Yonsei University, Seoul 120-749, Republic of Korea.

<sup>3</sup> To whom correspondence should be addressed (email paiky@yonsei.ac.kr).

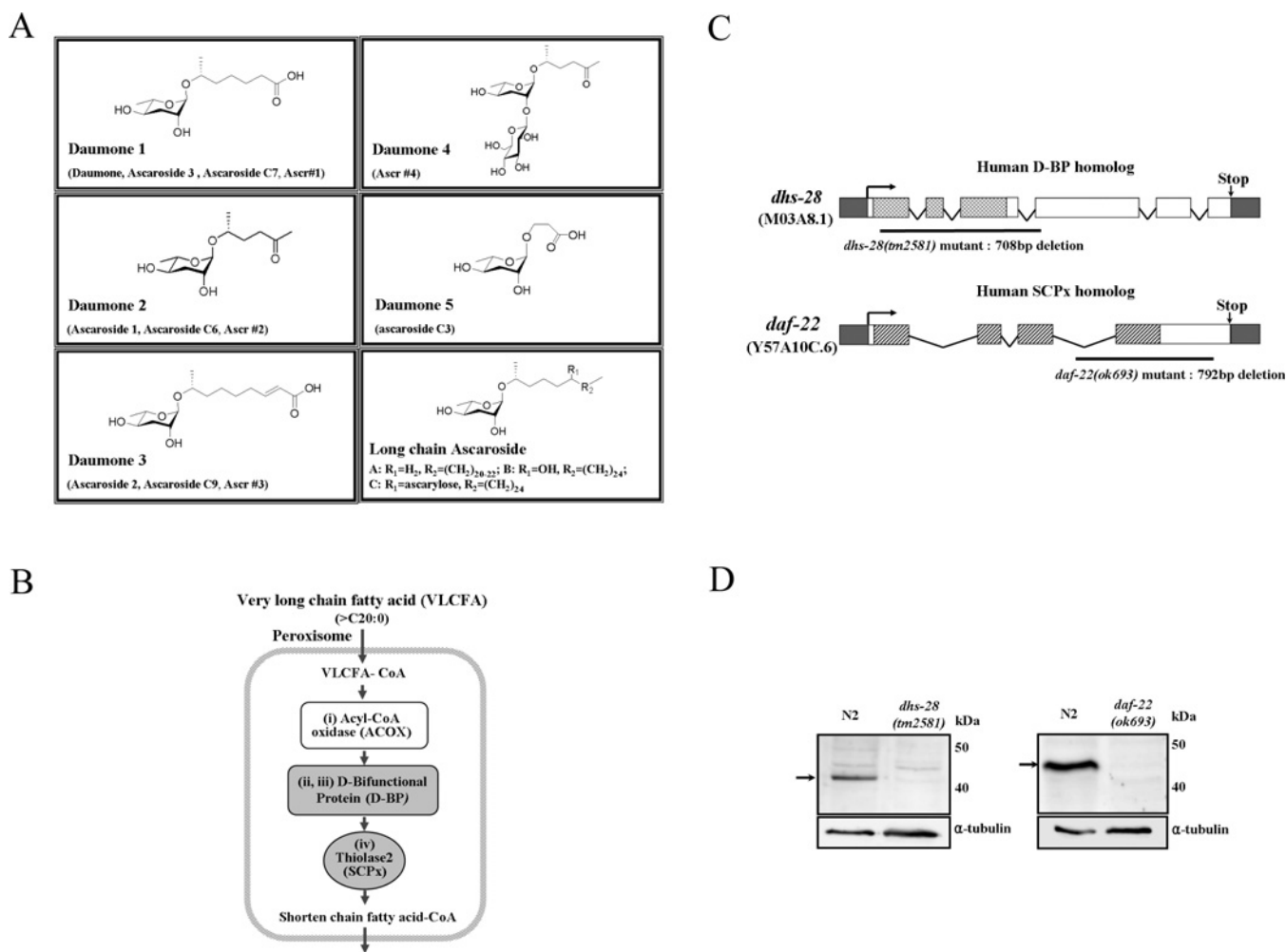


**Figure 1** Structural and functional components related to daumone biosynthesis

(A) Structures of the five known dauer pheromones, with different proposed nomenclatures in the literature in parentheses [10–12,23], and three long-chain ascarosides in the nematode *Parascaris equorum* [14]. (B) Reaction sequence of peroxisomal  $\beta$ -oxidation in mammals. (C) Structural organization of the *C. elegans* *dhs-28* and *daf-22* genes; underlines indicate deletions in corresponding mutants *dhs-28(tm2581)* and *daf-22(ok693)*. The catalytic domain of DHS-28 (▨) containing a short-chain dehydrogenase and hydratase (SDR) domain and DAF-22 (▧) containing a thiolase domain are shown. (D) Confirmation of the DHS-28 and DAF-22 protein in each *C. elegans* mutant by Western blot analysis. Following SDS/PAGE analysis of lysates obtained from N2 and the mutant worms, the gels were transferred to nitrocellulose membranes for immunoblotting using the corresponding antibody raised against the recombinant proteins of DHS-28 and DAF-22 respectively (left panel: anti-DHS-28 antibody, right panel: anti-DAF-22 antibody, prepared as described in the Experimental section). Anti- $\alpha$ -tubulin antibody (bottom of each panel) was used as an internal control. The sizes of molecular mass standard proteins are indicated on the right.

peroxisome is also known to metabolize certain VLCFA-derived lipophilic caboxylates (e.g. bile acid intermediates, eicosanoids, and fat soluble vitamins E and K) by excreting them out of the body [24], indicating its potential contribution to cellular homeostasis.

In the present study, we addressed one important question pertaining to the daumone biosynthesis pathway. What are the physiological consequences of (impaired) peroxisomal  $\beta$ -oxidation of the VLCFAs, or their fatty acyl-CoAs expected to be involved in the production of the various aglycone units ( $<C_9$ -SCFA) for daumone biosynthesis? To answer this question, we first elaborated the mechanism whereby daumone biosynthesis is carried out and then closely examined the impact of deficiency in daumone biosynthesis using the two enzymes, DHS-28 and DAF-22 [22] [formally called SCPx (sterol carrier protein x)] [23], involved in peroxisomal  $\beta$ -oxidation of VLCFAs and *C. elegans* mutants defective for these enzymes. Here we show daumone biosynthesis requires peroxisomal  $\beta$ -oxidation and is

an essential detoxification process for some of the harmful peroxisomal fatty acids which otherwise can be routinely used for daumone biosynthesis throughout the life cycle in *C. elegans*.

## EXPERIMENTAL

### Strains

*C. elegans* strains were maintained on NGM agar plates at 20°C as described previously in [25]. The N2 Bristol strain was used for all experiments unless otherwise noted. Worms were fed *E. coli* strain OP50 unless otherwise stated. All of the mutant strains used in this study were obtained from the *Caenorhabditis* Genetics Center (Minneapolis, MN, U.S.A.) and NBRP (Tokyo, Japan). The strain containing [p<sub>HSP16/2</sub>:GFP (green fluorescent protein)-SKL] was kindly provided by the Monica Driscoll laboratory (Department of Molecular Biology and Biochemistry, Rutgers University, Piscataway, NJ, U.S.A.).

### Preparation of recombinant DHS-28 and DAF-22 and their polyclonal antibodies

cDNAs of *dhs-28* and *daf-22* genes were synthesized using mRNA isolated from N2 worms by PCR. The resulting cDNA fragments were cloned into a pET-28b expression vector (Invitrogen). *E. coli* BL21 cells harbouring the cloned pET-28b were cultured at 37°C. The cells were harvested and sonicated in lysis solution. SDS/10% PAGE analysis was carried out using cell lysates prepared by centrifugation at 11000 g for 5 min at 4°C. The protein bands corresponding to the appropriate gene products (~200 µg) were excised and used for polyclonal antibody preparation against recombinant DHS-28 and DAF-22 in rabbits inoculated three times with each protein in Freund's adjuvant during an 8-week period (AB Frontier, Seoul, Korea).

### Western blotting

Mixed N2, *dhs-28(tm2581)* and *daf-22(ok693)* worms were washed from NGM plates using S-basal buffer (all buffers used in the present study are described in Supplementary Table S1 at <http://www.BiochemJ.org/bj/422/bj4220061add.htm>). After washing the worms with the S-basal buffer three times, the buffer was also removed. The worms were mixed with 2 × sample loading buffer and boiled for 15 min. The resulting lysate was electrophoresed on a SDS/10% PAGE gel and the gel was transferred to a nitrocellulose membrane. The membrane was then incubated in blocking buffer containing anti-DHS-28 or anti-DAF-22 anti-rabbit antibody (1:1000 dilution) or anti-tubulin anti-mouse antibody (1:5000) at 4°C overnight, then in the blocking buffer containing anti-rabbit or anti-mouse horseradish peroxidase antibody (1:5000 dilution) at 25°C for 1 h. Secondary antibodies on the membrane were detected with an enhanced chemiluminescence Western blotting analysis system (Thermo Fisher Scientific, Inc.); luminescence was captured with an LAS-3000 imaging system (Fujifilm).

### Construction and expression of DHS-28-GFP and DAF-22-GFP

Each PCR-directed amplified DNA fragment encompassing the *dhs-28* and *daf-22* full gene was ligated into the GFP cassette pPD114.108 kindly provided by Professor A. Fire (Departments of Pathology and Genetics, Stanford University School of Medicine, Stanford, CA, U.S.A.). For construction of the *dhs-28Prom::GFP::dhs-28* full gene, PCR amplification was performed with *C. elegans* genomic DNA to obtain a 1.556 kb promoter sequence upstream of the first codon of *dhs-28*, and the resulting DNA fragment was ligated into the PstI/BamHI restriction site located upstream of the GFP protein of the pPD114.108 GFP vector. All exons and introns of *dhs-28* (1.545 kb) amplified by PCR were ligated into the EcoRI/NheI site downstream of the GFP-coding region. For construction of the *daf-22Prom::GFP::daf-22* full gene, a sequence 1.530 kb upstream of *daf-22* (promoter portion) was amplified by PCR and the resulting DNA fragment was ligated into the XbaI/NotI restriction site upstream of the GFP-coding region of the pPD114.108 GFP vector. The entire coding region of *daf-22* (2.083 kb) was ligated into the NheI/ApaI restriction site downstream of the GFP-coding region. Approx. 100 µg/ml of *dhs-28Prom::GFP::dhs-28* full gene and *daf-22Prom::GFP::daf-22* full gene construct were injected into N2 worms, and progenies expressing GFP were selected.

### Liquid culture and plate daumone assays for dauer induction

*C. elegans* were cultured on 30 ml of S basal liquid medium containing MgSO<sub>4</sub>, CaCl<sub>2</sub>, cholesterol, streptomycin and *E. coli*

(OP50) for 10 days at 20°C. To induce a high population density (> 50000 worms/ml), additional *E. coli* was added to media at the fourth to fifth day. The number of dauers in the liquid was counted after 10 days. Dauer larvae were confirmed by treatment with 1% SDS solution for 40 min as described previously [1]. The plate dauer assay was performed as described previously in [2].

### Purification and quantification of various dauer pheromone species

*C. elegans* was cultured on S basal liquid medium in a 6 litre fermenter for 10 days at 20–23°C on *E. coli* (OP50). The series of organic solvent extractions of both culture broth and worm bodies were carried out using the methods previously described in [2]. The final ethyl acetate fractions were then cleaned with a silica-gel column (100 × 10 cm) previously equilibrated with hexane/ethylacetate/methanol (7:7:1, by vol.); the bound fractions were then eluted with methanol. Daumones in bound and unbound fractions were analysed by LC (liquid chromatography)-MS/MS (tandem MS) in a LTQ mass spectrometer (Thermo Scientific) equipped with an ESI (electrospray ionization) source. The LC separation of daumones was performed in an Agilent 1200 LC system housing an XTerra C<sub>18</sub> column (2.0 × 150 mm, 3.5 µm particles; Waters). The flow rate of the mobile phase (gradient described in Supplementary Table S2 at <http://www.BiochemJ.org/bj/422/bj4220061add.htm>) was 0.2 ml/min. For selective and reliable quantification of daumone species, SRM (selected reaction monitoring) was used. Fragmentations of (M+NH<sub>4</sub>)<sup>+</sup> precursor ions of daumones into selective product ions resulting from concomitant loss of ammonia and ascarylose units were used as SRM channels (see Supplementary Figure S4A).

### Analysis of fatty acids and fatty acyl-CoAs in worms

For quantitative analysis of the fatty acid composition, worms were washed with the S-basal buffer three times and the buffer was also removed. FA methyl esters were prepared as described [26]. As an internal standard, 0.5 mg of pentadecanoic acid (C<sub>15:0</sub>) was added to the worm samples. Approx. 1.0 ml of 2.5% methanolic H<sub>2</sub>SO<sub>4</sub> was then added, and the worm samples were heated for 1 h at 90°C. After cooling the samples, 1.0 ml of hexane and 1.5 ml of H<sub>2</sub>O were added and mixed thoroughly. Methyl esters of fatty acids were extracted into the hexane layer (upper phase) by shaking and centrifuging at low speed. Methyl esters in the hexane layer were analysed using an Agilent HP6890 GC (gas chromatograph)-HP5973N MSD (mass selective detector) system (Agilent) equipped with an HP-5 column (30 m × 0.25 mm, 0.25 µm). Three replicates of fatty acid methyl esters were prepared and analysed for each of the three worms: N2, and *dhs-28* and *daf-22* mutants. Analysis and extraction of fatty acyl-CoA was carried out using the protocol given by Haynes et al. [27] with slight modification. Briefly, approx. 4.0 ml of CH<sub>3</sub>OH (containing 1 mM EDTA) was added onto the worm sample along with 10 µM of pentadecanoyl-CoA as an internal standard. To this mixture, 2.0 ml of CHCl<sub>3</sub> was added and sonicated. After the reaction mixture was incubated for 1 h at 50°C, 2.0 ml of CHCl<sub>3</sub> and distilled water were added and vortexed thoroughly. The reaction mixture was centrifuged briefly, and the upper aqueous phase was collected for LC-MS/MS analysis. The same LC-MS system used for the daumone analysis was operated in the negative ESI mode for LC-MS/MS analysis of fatty acyl-CoAs in N2, *dhs-28* and *daf-22* worms.

### qRT-PCR (quantitative reverse transcription-PCR)

qRT-PCR was performed according to the method of Jeong et al. [9]. cDNA was synthesized using mRNA isolated from

worms at each stage. PCR was performed using the SYBR Green PCR Master Mix (Qiagen) according to the manufacturer's instructions, and reactions were run on a DNA Engine Opticon® 2 System (MJ Research). Relative expression rate (%) was determined using the  $\Delta C_t$  method, and an average of the expression of the reference gene *act-1* was used to control for template levels. Each experiment was performed in triplicate.

### Growth rate, body size, brood size and lifespan measurement

To measure the growth rate, five synchronized adult worms were transferred to the fresh NGM (nematode growth medium) plate to lay eggs for 2 h. The worms were removed and their progeny was grown at 20°C. At 72 h, we counted the number of worms at each developmental stage. The developmental stage was determined according to germ cell number, vulva development and body length (wormatlas, <http://www.wormatlas.org/>). The measurement of body size (body length and width) was performed as described in [28], and the brood size determined as previously described [29]. Lifespan assay was carried out according to the method described in [30].

### Fat staining

Sudan Black staining was performed as described in [31]. Animals grown on the unstarved plate were washed with M9 or PBS buffer and fixed with 1% paraformaldehyde. The worms were then subjected to three freeze–thaw cycles and dehydrated through an ethanol series (25%, 50%, 70%). Then, 2–5 vol. of Sudan Black B solution were added to the worms, which were then incubated for 30 min, washed with 25% ethanol twice, and photographed. Nile Red and C1-BODIPY-C12 staining was performed as described in [32]. Stock solutions of Nile Red powder (Molecular Probes) in acetone (0.5 mg/ml) and C1-BODIPY-C12 (Molecular Probes) in DMSO (5 mM) were freshly diluted in 1 × PBS and added on top of NGM plates seeded with OP50. Final concentrations were 0.05 µg/ml (Nile Red) and 1 µM (C1-BODIPY-C12). Synchronized eggs were transferred to the dye-containing plates and incubated; worms at the same stage were then collected and observed under a fluorescence microscope with the same exposure time.

## RESULTS

### *C. elegans* daumone is derived from *de novo* ascarylose synthesis

Before we investigated the main question as to the physiological impact of deficiency in dauer pheromone biosynthesis, it was necessary for us to clarify a couple of questions: i) what is the origin of ascarylose (*de novo* synthesis versus being obtained from *E. coli*); and ii) how does the peroxisomal  $\beta$ -oxidation contribute to daumone biosynthesis? To answer the first question as to the origin of ascarylose, N2 worms were fed two K-12 *E. coli* mutants (instead of OP50) known to be deficient in ascarylose biosynthesis genes *ascB* (JW2686) and *ascF* (JW5435) (<http://www.shigen.nig.ac.jp/ecoli/strain/top/top.jsp>). Worms were grown in S medium culture broth for 10 days, and the assay for dauer induction was performed as described [1]. As shown in Supplementary Figure S1 (at <http://www.BiochemJ.org/bj/422/bj4220061add.htm>), worms grown in the presence of both mutant *E. coli* strains entered the dauer state quite well (OP50 fed group: 23 ± 2.0%, JW2686: 25 ± 3.4%, JW5435: 20 ± 2.5%), indicating that ascarylose production in *E. coli* is not required for daumone biosynthesis by *C. elegans*.

### Peroxisomal expression of candidate daumone biosynthetic genes

In answer to the second question as to the method of the contribution of the peroxisomal  $\beta$ -oxidation (Figure 1B) pathway for providing fatty acid side chains to daumone biosynthesis, we anticipated part of the dauer pheromone would go through the typical four step reactions shown in Figure 1(B), which are composed of first dehydrogenation by ACOX (acyl-CoA oxidase) [reaction (i)], hydration [reaction (ii)] plus a second dehydrogenation [reaction (iii)] by D-BP (D-bifunctional protein) and final thiolytic cleavage by SCPx (now called DAF-22 [22] in *C. elegans* [23]), reaction (iv) (Figure 1B) [33]. An attempt was made to identify potential target genes for the daumone biosynthesis pathway by screening *C. elegans* homologous genes corresponding to the enzymes involved in the predicted peroxisomal  $\beta$ -oxidation [ii–iv] (Figure 1B) through NCBI (<http://www.ncbi.nlm.nih.gov/>) and PSORT II databases (<http://psort.ims.u-tokyo.ac.jp/>). We identified homologous genes encoding a *C. elegans* orthologue of a human D-BP (D-bifunctional protein) homologue, named DHS-28, and a *C. elegans* orthologue for a human SCPx homologue, named DAF-22 (also known as 3-ketoacyl CoA thiolase2-pTH2), encoded by the Y57A10C.6 (Supplementary Figure S2 at <http://www.BiochemJ.org/bj/422/bj4220061add.htm>). Based on the availability of mutant strains, we focused on three (ii–iv) of four consecutive reactions involving the synthesis of daumone aglycones  $\leq C_9$  from VLCFAs, as predicted to be catalysed by DHS-28 and DAF-22 (Figures 1B and 1C). We employed two mutant *C. elegans* strains, *dhs-28(tm2581)*, containing a mutation of the *dhs-28* gene (provided by NBRP) and *daf-22(ok693)* [22] (from CGC, Minneapolis, MN, U.S.A.), containing a mutation of *daf-22* for this study (Figure 1C). These had been out-crossed with N2 six times to remove possible unrelated mutations. To confirm the deletions in the structural sequences of DHS-28 and DAF-22 in the mutants, Western blotting was performed with polyclonal antibodies against each wild-type recombinant protein (see the Experimental section). As anticipated, the expected protein bands of DHS-28 and DAF-22 disappeared in the gene products of *dhs-28(tm2581)* and *daf-22(ok693)* (Figure 1D). To gain further information as to the tissue-specific gene expression pattern of both DHS-28 and DAF-22, both *dhs-28Prom::GFP::dhs-28* full gene and *daf-22Prom::GFP::daf-22* full gene were injected into N2 worms, and the GFP expression in their progenies was observed (Figure 2). They showed the same expression as punctate patterns in both hypodermis and intestine cells. When worms were subjected to *prx-5* RNAi (RNA interference), which mediates import of peroxisomal proteins from the cytosol [33], the expression of both DHS-28–GFP and DAF-22–GFP was turned into a dispersed pattern, suggesting that they are *bona fide* peroxisome-localized proteins (Figure 2).

### *dhs-28* and *daf-22* mutants do not synthesize daumone

We examined whether *dhs-28(tm2581)* and *daf-22(ok693)* mutants were able to synthesize, secrete and sense daumones by dauer assays as well as chemical analysis. N2, *dhs-28(tm2581)* and *daf-22(ok693)* were cultured in S broth for 10 days at 20°C, during which food in the form of *E. coli* was added at day 4 to day 5 to increase the population density. We performed plate dauer assay using the crude daumone extracts obtained from the culture broth of N2, *dhs-28(tm2581)* and *daf-22(ok693)*. In this assay, N2 worms grown on the NGM plate in the presence of crude pheromone extracts of N2 worms produced approx. 80% dauer population, whereas N2 worms that were placed in the presence of crude pheromone extracts from either *dhs-28(tm2581)* or *daf-22(ok693)* showed no dauer

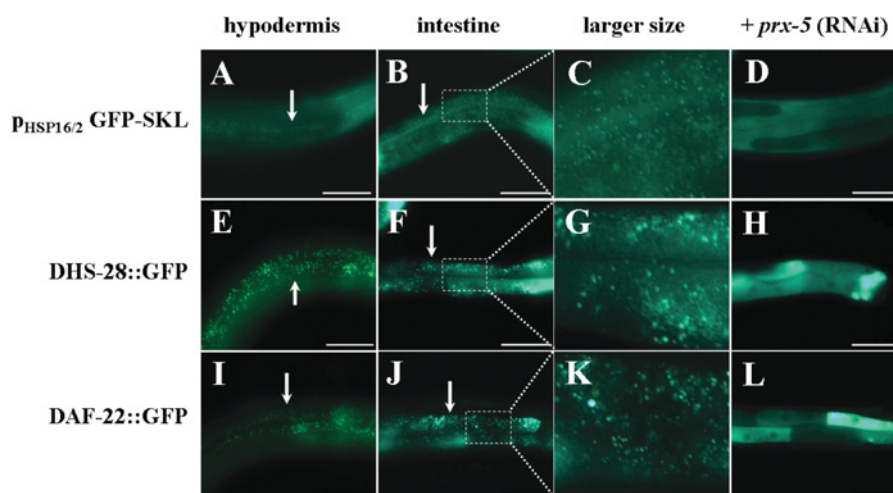


**Figure 2** DHS-28 and DAF-22 are located in peroxisomes of the hypodermis and intestinal cells

The plasmid vector for *dhs-28Prom::GFP::dhs-28* full gene and *daf-22Prom::GFP::daf-22* full gene were constructed and injected into wild-type N2 worms.  $p_{HSP16.2}GFP-SKL$  (a gift from Professor M. Driscoll), a peroxisomal-localizing control vector, was injected into N2 (**A**, **B** and **C**) [33]. The expression of DHS-28::GFP (**E**, **F** and **G**) and DAF-22::GFP (**I**, **J** and **K**) in hypodermis and intestine is shown, with enlargements of intestinal expression (**C**, **G** and **K**). Far right panels show that *prx-5* RNAi treatment abolished peroxisomal expression of  $p_{HSP16.2}GFP-SKL$  (**D**), DHS-28::GFP (**H**) and DAF-22::GFP (**L**). Scale bar = 50  $\mu m$ .

phenotype at all (Supplementary Figures S3A and S3B at <http://www.BiochemJ.org/bj/422/bj4220061add.htm>). We also determined whether the mutants could perceive dauer pheromones by performing plate dauer assays using pure synthetic daumone 1 [2]. The N2 strain produced > 90% dauer larvae, whereas *dhs-28(tm2581)* and *daf-22(ok693)* showed only half of the wild-type N2 [i.e.  $47.7 \pm 1.2\%$  for *dhs-28(tm2581)* and  $43.6 \pm 4.7\%$  for *daf-22(ok693)*]. It was also observed that daumone signal sensing appears to be partially defective in these mutants (Supplementary Figure S3C). This result clearly indicates that *dhs-28(tm2581)* and *daf-22(ok693)* are incapable of synthesis and/or secretion of daumone.

Because the specific cause of the dauer-defective phenotype in the mutants, blocked secretion or impaired biosynthesis, remained unresolved, we measured the production of daumones in each mutant strain. In this experiment, N2, *dhs-28(tm2581)*, and *daf-22(ok693)* were grown in a 6 litre fermenter for 10 days, then culture broth and worm body fractions were prepared. These fractions were purified by a series of organic extraction procedures followed by silica gel column chromatography to isolate each daumone, and the isolates were subjected to LC-MS/MS analysis for quantification as previously described [2] (Supplementary Figure S4 and Supplementary Table S2 at <http://www.BiochemJ.org/bj/422/bj4220061add.htm>). In addition, daumones 1–3 were chemically synthesized; their chemical structures were verified by their NMR spectra and quantified using appropriate standard curves (Supplementary Figures S4 and S5). In the culture broth of N2, daumone 2 was predominant (approx.  $1.918 \mu M$ ), followed by daumone 1 ( $0.156 \mu M$ ) and daumone 3 ( $0.079 \mu M$ ) (Figure 3). This result differed somewhat from that previously published [10], where daumone 2 was also the most abundant but daumone 1 was the least abundant. This could be due to differences between the two groups in detection methods (LC-MS compared with NMR), daumone preparation procedures, or *C. elegans* culture conditions [10]. Nevertheless, it is confirmed again that daumone 2 is the predominant form of daumone present in *C. elegans*. Note that extracts of worm bodies or culture broth of *dhs-28(tm2581)* and *daf-22(ok693)* did not contain detectable daumone analogues (Figure 3 and

Supplementary Figure S4). This clearly indicates that these mutants are incapable of endogenous daumone biosynthesis and thus peroxisomal  $\beta$ -oxidation of VLCFAs is required for daumone biosynthesis.

#### Impaired peroxisomal $\beta$ -oxidation coupled to daumone biosynthesis causes massive accumulation of fatty acids inside the worm body

One of the remarkable phenotypes of both *dhs-28(tm2581)* and *daf-22(ok693)* was the massive accumulation of large fat granules in the intestines, which appeared much larger than those in wild-type N2 worms (Figure 4A). The number and size of fat granules tended to increase in prominence as development proceeded in *dhs-28(tm2581)* than in *daf-22(ok693)* (Figures 4A and 4B), suggesting its potential detrimental effects on the related fatty acid metabolism. This phenomenon was continuously detected throughout all developmental stages from larva to adult in both mutants (Supplementary Figure S6A at <http://www.BiochemJ.org/bj/422/bj4220061add.htm>). To confirm that these granules were actually composed of authentic fats, worms were stained with the lipid-specific stains Sudan Black, Nile Red and C1-BODIPY-C12. As shown in Figure 4(B), the granules (in the form of triacylglycerols) were stained well by each dye, and fat droplets in *dhs-28(tm2581)* appeared much denser and larger than those in *daf-22(ok693)*. When *dhs-28(tm2581)* or *daf-22(ok693)* were rescued by injection of a *dhs-28* or *daf-22* full gene GFP vector, the fat granules were reduced or disappeared (Supplementary Figure S6B). To investigate which type(s) of fatty acid or fatty acyl-CoA accumulated in mutants, total fatty acids and their acyl-CoAs were extracted from wild-type N2 worms, *dhs-28(tm2581)* and *daf-22(ok693)* and then were analysed by either GC-MS (for fatty acid quantification) or LC-ESI-MS/MS (for fatty acyl-CoA quantification) (Supplementary Figure S7 and Supplementary Table S3 at <http://www.BiochemJ.org/bj/422/bj4220061add.htm>). In the case of VLCFAs, both *dhs-28(tm2581)* and *daf-22(ok693)* contained approx. 1.5- to 3.8-fold the molar levels of specific fatty acids

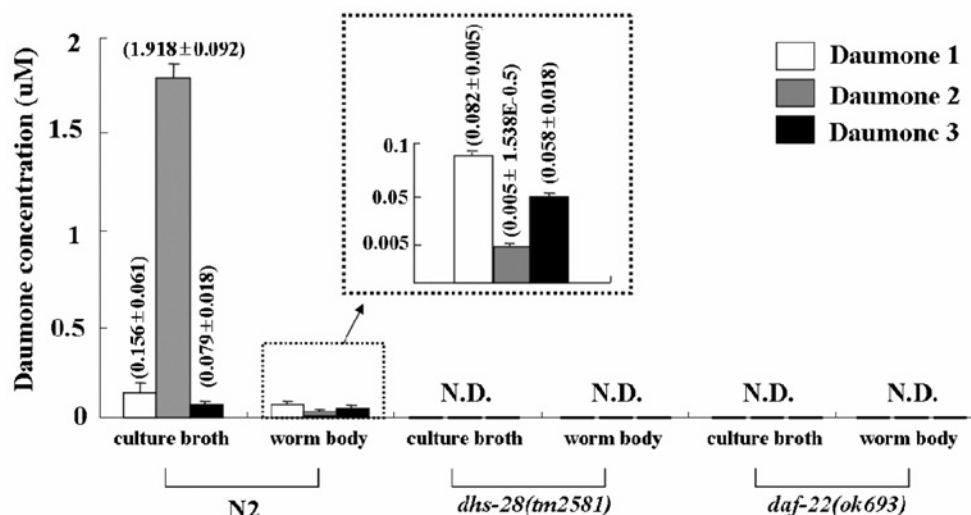


**Figure 3** *dhs-28(tm2581)* and *daf-22(ok693)* are defective in dauer pheromone biosynthesis

Quantification of dauer pheromone produced from culture broths and worm body fractions of N2, *dhs-28(tm2581)* and *daf-22(ok693)*. The concentration of each dauer pheromone was determined using LC-MS/MS by interpolating or extrapolating from standard curves prepared from synthetic daumones (Supplementary Figure S4). Values represent means ± S.D. from three independent measurement sets. Concentrations (μM) from N2: [culture broth (± S.D.): Daumone 1, 0.156 ± 0.061; Daumone 2, 1.918 ± 0.092; Daumone 3, 0.079 ± 0.018. Worm body (± S.D.): Daumone 1, 0.082 ± 0.005; Daumone 2, 0.005 ± 1.538E<sup>-05</sup>; Daumone 3, 0.058 ± 0.018]. N.D., not detected.

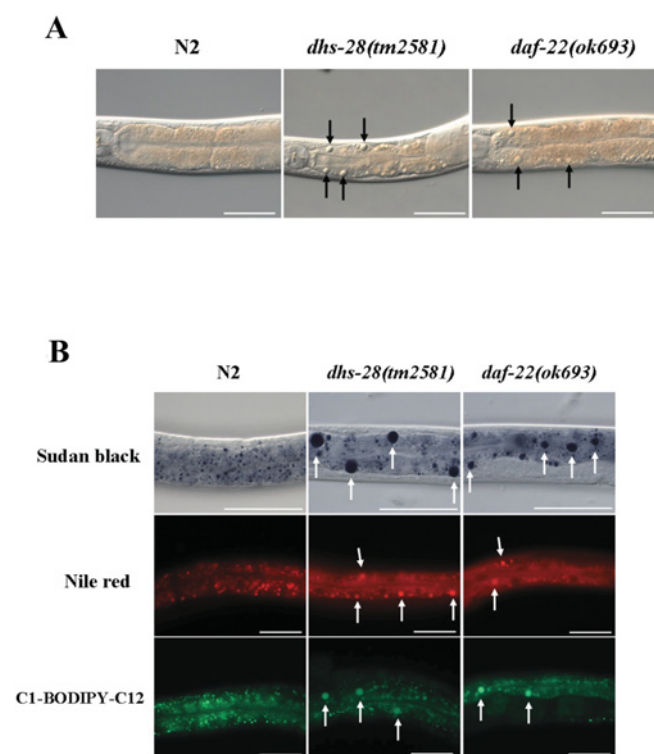


**Figure 4** Fat granule phenotype in the intestines of *C. elegans* N2, *dhs-28(tm2581)* and *daf-22(ok693)*

(A) Phenotype of fat granules in young adult N2, *dhs-28(tm2581)* and *daf-22(ok693)*. Huge fat granules can be seen in intestine of both *dhs-28(tm2581)* and *daf-22(ok693)*. Scale bar, 50 μm. (B) Staining of fats with various dyes: Sudan Black, Nile Red and C1-BODIPY-C12. Arrowheads show the granules. Fat staining was performed with L4-young adults of the N2 and each mutant strain. Scale bar = 50 μm.

with chain lengths higher than C<sub>20</sub> compared to N2 (Figure 5A). For fatty acyl-CoAs, *daf-22(ok693)* mutants showed an even higher rate of accumulation (7- to 100-fold) of VLCFAs (>C<sub>21</sub>) compared with that in N2 (Figure 5B). It should be noted that the fatty acids shown in Figures 5(A) and 5(B) represent only those having >C<sub>14</sub> for the purpose of comparison among various fatty acids in *C. elegans*. Collectively, these data suggest that mutation of these two genes directly causes massive accumulation of acyl-CoAs of VLCFAs (Figure 5B). In *E. coli* (OP50), there was essentially no VLCFAs longer than C<sub>20</sub> (Supplementary Figure S7B), confirming that all VLCFAs detected were more likely synthesized in *C. elegans*.

#### Consequences of deficiency in daumone biosynthesis in postembryonic development and lifespan

To investigate the expression pattern of *dhs-28* and *daf-22* genes, their mRNA levels were measured using qRT-PCR. Both genes were expressed similarly; their expression levels peaked at the L3 stage and decreased as worms developed to the adult stage (Figure 6A), indicating their important roles in the later stage of development. Even more, it has been previously reported that RNAi-mediated gene silencing of those genes related to peroxisome biogenesis and metabolism caused serious defects in post-embryonic development [33,34]. We therefore wanted to investigate the effects of mutation of *dhs-28* and *daf-22* on post-embryonic development. We observed that there was a significant reduction in the growth rate (percentage of worms from egg to adult) of *daf-22(ok693)* (6.1% ± 4.6) as compared with that of N2 (93.8% ± 2.2). There were almost no worms grown to adult in *dhs-28(tm2581);daf-22(ok693)* (0%) and *dhs-28(tm2581)* (0%), (Figure 6B and Supplementary Table S4 at <http://www.BiochemJ.org/bj/422/bj4220061add.htm>). Furthermore, young adults of *daf-22(ok693)* were 8% shorter and 12% narrower than those of N2, whereas young adults of

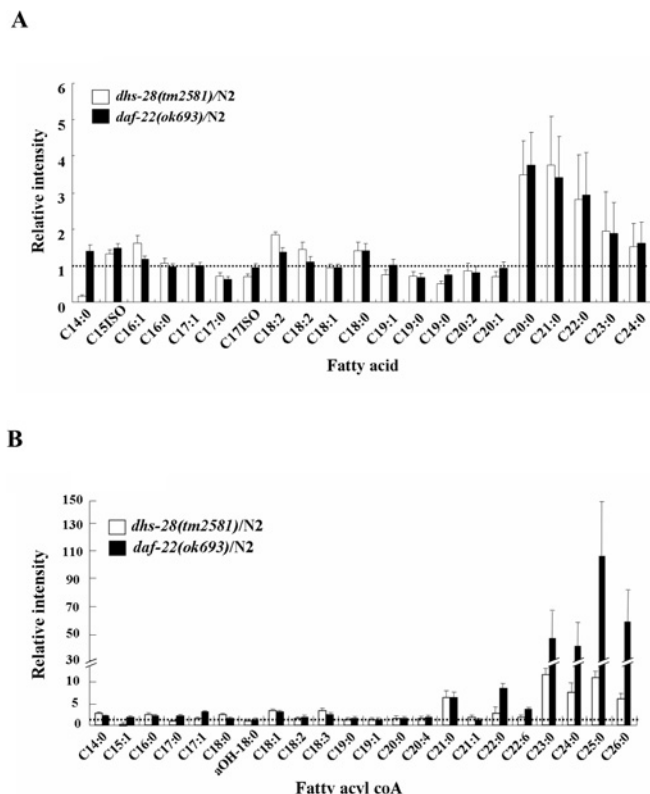


**Figure 5** Quantitative analysis of accumulated fatty acids in *C. elegans* *dhs-28(tm2581)* and *daf-22(ok693)* relative to N2

(A) Fatty acid distribution profiles for *dhs-28* and *daf-22* mutants relative to those for N2 wild-type were obtained by GC-MS analysis. (B) Fatty acyl-CoA distribution profiles for *dhs-28(tm2581)* and *daf-22(ok693)* mutants relative to those for N2 wild-type were obtained by LC-MS/MS analysis. Values represent means  $\pm$  S.D. from three independent experimental sets; dotted line indicates a relative ratio between the mutants and N2 of 1.0.

*dhs-28(tm2581)* were 13% shorter and 18% narrower than N2 young adults (Figure 6C). Brood sizes of these two mutants were also substantially reduced (up to > 40%) (Figure 6D).

To examine if these detrimental effects caused by accumulation of peroxisomal unprocessed VLCFAs or their acyl-CoAs might shorten the lifespan of these mutants, an MLS (mean lifespan) and XLS (maximum lifespan) of these two mutants that had been grown in NGM plates were determined. We found that they showed approx. 14 to 30% reduction in lifespan (e.g. MLS, 14.2 days for *dhs-28(tm2581)*; 17.3 days for *daf-22(ok693)*, 20.3 days for N2) (Figure 6E), implying that the accumulation of peroxisomal non-permissible VLCFAs culminated in a detrimental effect on lifespan (Figure 7A).

## DISCUSSION

In the present study, we provide evidence that the daumone glycone unit (ascarylose) is synthesized endogenously and is not obtained from *E. coli*, and that peroxisomal  $\beta$ -oxidation is tightly coupled to biosynthesis of the aglycone moiety in a developmentally important process in *C. elegans*. Although it remains possible for *C. elegans* to obtain ascarylose from *E. coli* if the latter contains a full suite of ascarylose synthesis genes, similar to other micro-organisms [21], our data on feeding *E. coli* mutants deficient in ascarylose synthesizing genes (e.g. *ascB* and *ascF*, Supplementary Figure S1) to *C. elegans* confirms that *C. elegans*

can biosynthesize ascarylose *de novo*. This is also indicated by a recently released database (BLASTP 2.2.19+, UniProt release 14.7, Jan 20, 2009), in which *C. elegans* appears to contain at least three genes homologous to *Y. pseudotuberculosis ascB* genes (C01F1.3, F56H6.5, F53B1.4) and two genes homologous to bacterial *ascF* (F53B1.4 and C01F1.3). We also established that DHS-28 and DAF-22 [22,23], major subjects of this study, are required for daumone biosynthesis.

Biosynthesis of daumone in *C. elegans* apparently implies two important contributions to cellular homeostasis. First, it provides a means for *C. elegans* to excrete a neuroendocrine sensory signal (pheromone) that transmits a nutritional or environmental state to physiological response at L2, leading to a decision as to whether they enter the dauer state or not for long-term survival in the unfavourable growth condition. Secondly, it offers one way of detoxification by converting peroxisomal fatty acids that otherwise would be accumulated (no excretion) into readily excretable fatty acid-ascarylose conjugates (ascarosides) (Figure 7A). However, there remain a few questions that need to be addressed. First, what is the relationship between daumone biosynthesis and detoxification in *C. elegans*? Secondly, do these two enzymes, DHS-28 and DAF-22, undertake two distinct reactions (daumone biosynthesis and detoxification) or one reaction process which has two functions? Although daumone biosynthesis could be one of many metabolic reactions which share common peroxisomal  $\beta$ -oxidation (e.g. bile acid), our data suggest that daumone biosynthesis is more likely a part of a detoxification process during which one of the UGTs (UDP-glucuronyltransferases) is predicted to catalyse conjugation between toxic SCFAs (mostly methyl branched fatty acids) and ascarylose to produce excretable daumones (Figure 7B). UGT is a well known detoxification enzyme in eukaryotes and synthesizes various sugar conjugates of lipophilic molecules (e.g. fatty acids and steroids) that can be easily excreted to outside cells [35,36]. For instance, it was recently reported that when *C. elegans* was exposed to organophosphates and neurotoxic agents, the *ugt* gene was one of the highly induced genes [37]. It is also well known that the last part of  $C_{24}$ -bile acid biosynthesis occurs in the peroxisome where sterol side chains are shortened, as seen in the case of VLCFAs for daumone biosynthesis [38]. Recently, *in vitro* studies showed that  $C_{27}$  bile acid intermediates (unprocessed precursors of  $C_{24}$ -bile acid) were found to be toxic (i.e. decrease cell viability and energy production, increase reactive oxygen species) [39]. Taken together, daumone biosynthesis appears to be a part of a common detoxification process in which DHS-28 and DAF-22 are actively involved in the course of fatty acid-derived energy production. Regarding the toxic aspect of daumone, Gallo and Riddle [40] reported that even optimal concentrations of daumone (e.g. 384  $\mu$ M) at which most dauer-inducing effect can be observed, caused some toxic effect on *dpy-14* mutants bearing defective cuticles. If a mutant-bearing deficiency in daumone transport were available, it would be interesting to determine whether accumulation of daumone itself inside the worm body would really cause any harmful effect. Thus, we conclude that daumone biosynthesis is one step that has two functions (production of pheromone and excretion of toxic waste) and *C. elegans* would utilize this reaction to dispose of toxic peroxisomal fatty acids for cellular homeostasis.

Since various long-chain ascarosides are known to occur in parasitic nematodes such as *Ascaris*, *Ascaridia galli* and *Parascaris equorum* [13–16,41] (Figure 1A), aglycones of these very-long chain ascarosides could be synthesized by Claisen-type condensation of two fatty acids and esterified with glycone in *Ascaris sum* [42] (in a form of CDP-ascarylose) that had been formed from glucose-1-phosphate [17]. Based on this

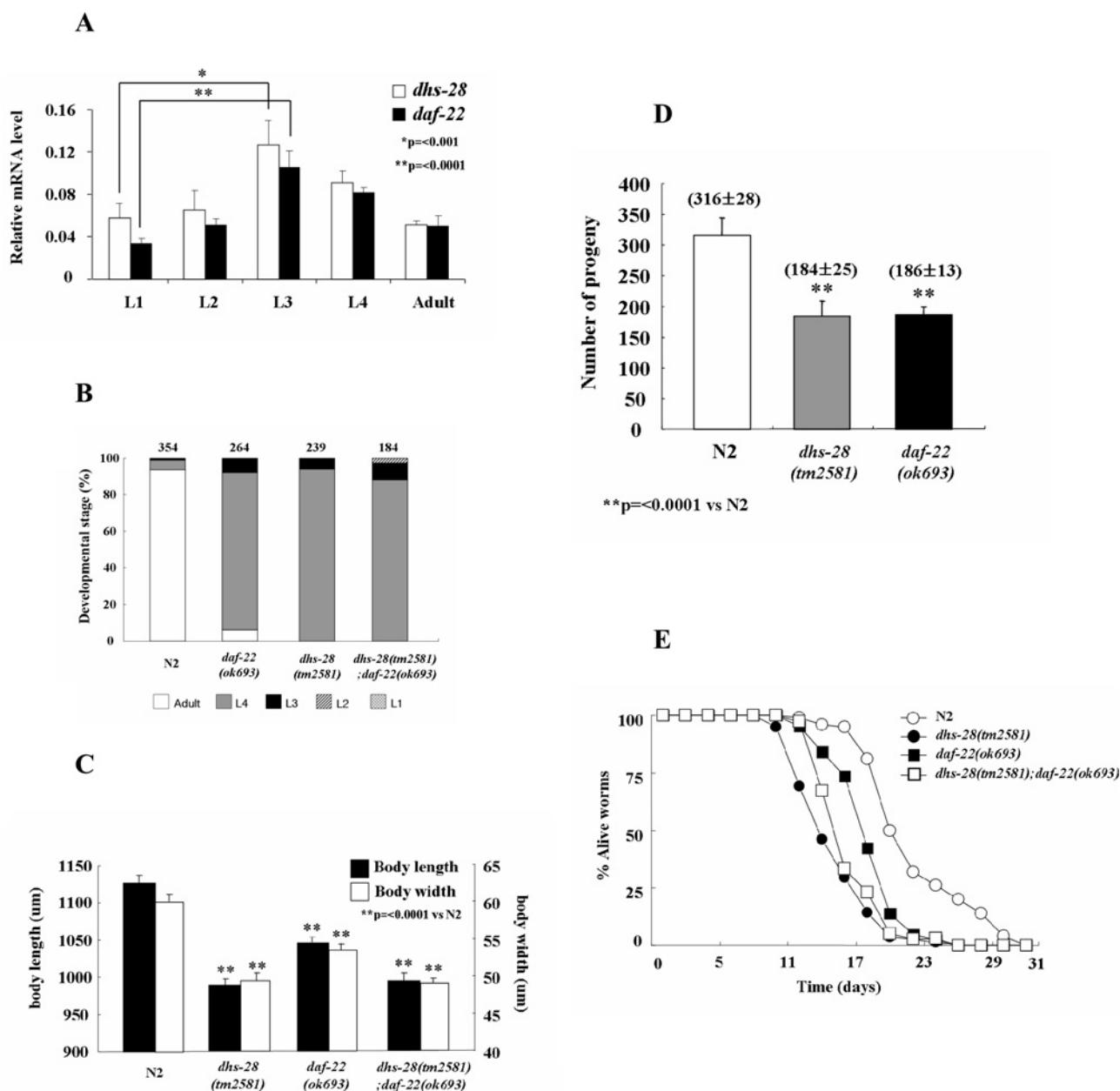


**Figure 6** Post-embryonic developmental defects of *C. elegans* mutants deficient in dauer pheromone biosynthesis

(A) The expression profile of mRNA level measured by qRT-PCR of *dhs-28* and *daf-22* genes in each stage of N2 worms. Values represent means  $\pm$  S.D. from three independent measurements. (B) Developmental growth rate (time of development from egg to adult) of N2, *dhs-28(tm2581)* and *daf-22(ok693)*. Worms were grown from synchronized eggs at 20 °C and the number of worms at each developmental stage was counted at 72 h. The total number of worms used in each group is shown at the top of the Figure (see Table S4 for statistical analysis). The results were from three independent experimental sets. (C) The body length (■) and body width (□) of N2, *dhs-28(tm2581)*, *daf-22(ok693)* and double mutants, *dhs-28(tm2581);daf-22(ok693)*, measured in 20 young adults of each strain. Values represent means  $\pm$  S.E.M. (D) Brood size of N2, *dhs-28(tm2581)* and *daf-22(ok693)*. Egg production from eight worms was monitored for 7 days. Values represent means  $\pm$  S.D. (E) Adult lifespan of *dhs-28(tm2581)*, *daf-22(ok693)* and *dhs-28(tm2581);daf-22(ok693)* grown in NGM. Mean lifespan  $\pm$  S.D. ( $n$  = worm number) was: N2, 21.4  $\pm$  1 ( $n$  = 84); *dhs-28(tm2581)*, 14.2  $\pm$  0.5 ( $n$  = 78); *daf-22(ok693)*, 17.3  $\pm$  0.9 ( $n$  = 87); *dhs-28(tm2581);daf-22(ok693)*, 15.8  $\pm$  0.5 ( $n$  = 74). Maximum lifespan  $\pm$  SD ( $n$  = number of worms) was N2, 30.3  $\pm$  0.7 ( $n$  = 84); *dhs-28(tm2581)*, 22.3  $\pm$  1.8 ( $n$  = 78); *daf-22(ok693)*, 22.3  $\pm$  1.3 ( $n$  = 87); *dhs-28(tm2581);daf-22(ok693)*, 21.0  $\pm$  1.2 ( $n$  = 77).  $P$  values compared with N2 were: 0.0003 for *dhs-28(tm2581)*, 0.0063 for *daf-22(ok693)*, and 0.0015 for *dhs-28(tm2581);daf-22(ok693)*. For each data point in Figure 6,  $P$  values were derived from  $t$  test.

information, one potential route of *de novo* daumone biosynthesis can be hypothesized. That is, daumone would be synthesized in intestinal cells in which expression of both *dhs-28* and *daf-22* is well confirmed (Figure 2). Once the ingested VLCFA enters a peroxisome of an intestinal cell, possibly by one of the ABC transporters [43], it would then be processed through peroxisomal  $\beta$ -oxidation, resulting in SCFAs which could be exported to the

cytosol, where they are esterified with an endogenous CDP-ascarylose, resulting in daumone (Figure 7B). With regard to export of the acetyl-CoA ( $C_2$ ), produced from each cycle of peroxisomal  $\beta$ -oxidation, it may be transported to either the cytosol or mitochondria as free acetate in carnitine ester form made by peroxisomal ACOT (acyl-CoA thioesterase) [44]. By analogy to acetyl-CoA, the incomplete oxidation products (i.e.

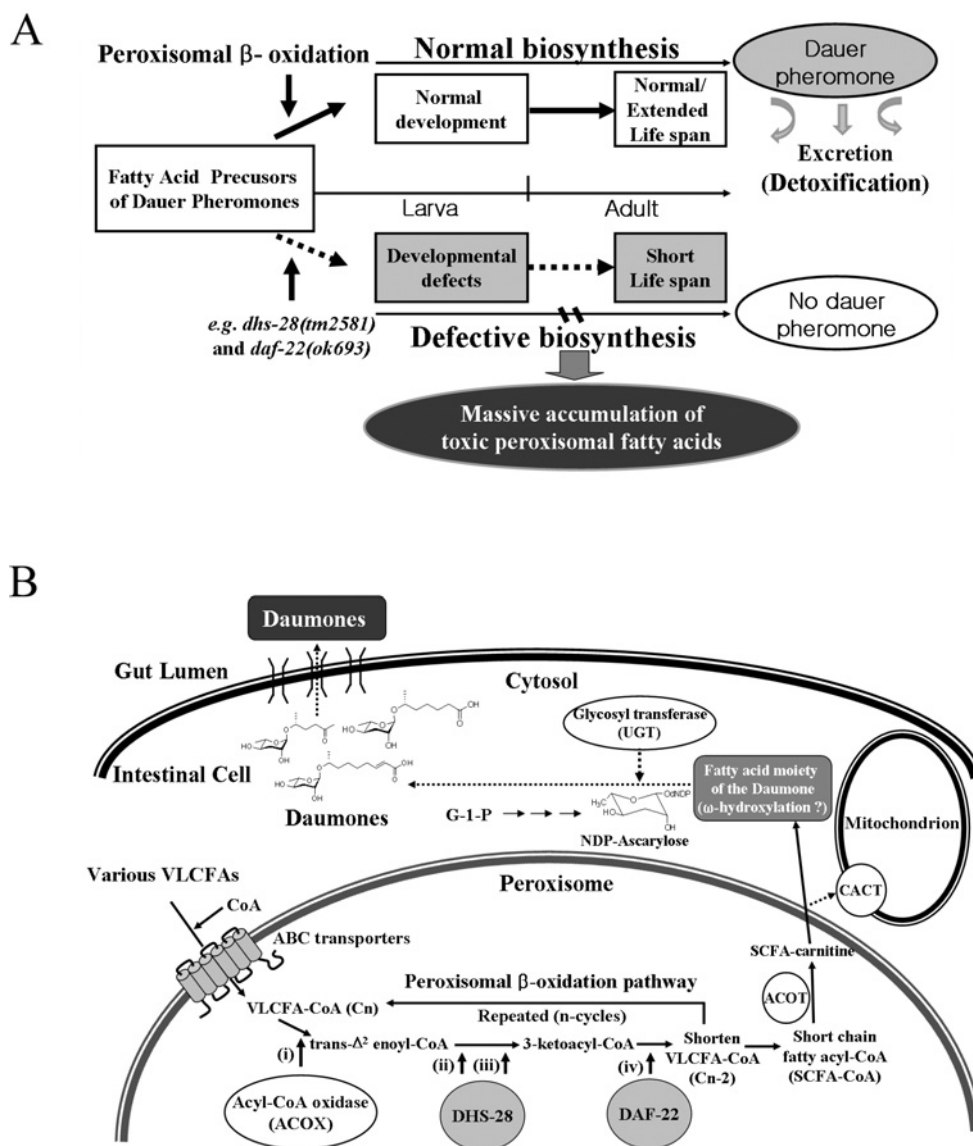


**Figure 7** Summary scheme of the impact of deficiency in daumone biosynthesis and possible routes for cellular daumone biosynthesis

(A) Disturbances in daumone biosynthesis through peroxisomal  $\beta$ -oxidation causes severe developmental defects. (B) Possible routes of complete daumone biosynthesis in *C. elegans* where many transporters and metabolizing enzymes are predicted to be involved.

SCFAs and their acyl-CoAs) from peroxisomal  $\beta$ -oxidation may be converted into carnitine esters by ACOT and moved out of the peroxisomes [44]. A question remains as to whether these carnitine esters of acyl-CoA would remain in the cytosol for daumone synthesis or be transferred to mitochondria by CACT (carnitine acylcarnitine translocase) encoded by *dif* [45] for another  $\beta$ -oxidation to produce either chain-shortened acyl-CoA or  $\text{CO}_2$ . In theory, if SCFAs or their acyl-CoAs were predominantly used for daumone synthesis by esterification with CDP-ascarylose by glycosyltransferase instead of being transported into the mitochondria for additional  $\beta$ -oxidation, then mitochondrial CACT would not have good substrate specificity for these  $\leq \text{C}_9$ -SCFAs and their acyl-CoAs. Given that the *dif* gene encoding CACT exists in *C. elegans*, it is reasonable to predict that *C. elegans* CACT may have much lower substrate specificity for these incomplete  $\leq \text{C}_9$  SCFAs or their acyl-CoAs, thereby resulting in poor mitochondrial uptake [46]. Thus, the acyl-CoAs

of these SCFAs may be hydroxylated by an unknown mechanism and then esterified with ascarylose to produce daumone in the cytosol (Figure 7B). Another possibility in this route is based on the observation of Verhoeven and Jakobs [47] that the incomplete peroxisomal  $\beta$ -oxidation products of  $\text{C}_{11}$ -SCFAs and their acyl-CoAs would be oxidized for only one cycle in the mitochondria to produce  $\text{C}_9$  SCFA or its acyl-CoA; therefore the latter SCFA or acyl-CoA would be eventually shuttled out to the cytosol where it would react with CDP-ascarylose to form daumone. This hypothesis remains to be validated.

Fatty acids and their acyl-CoAs have been regarded as a component of normal development because they are reversibly formed during regular developmental processes (e.g. dauer compared with post-dauer) and used for energy storage, membrane structure and various signalling pathways. However, in these mutants, VLCFA accumulation in the form of triacylglycerols originating from deficient peroxisomal  $\beta$ -oxidation

processes (Figure 5) appears to occur irreversibly and has been shown to be detrimental to *C. elegans* (Figure 6), e.g. VLCFA accumulation in liver, testis and nervous tissue of peroxisomal dysfunction mice causes pathophysiological defect [48]. In this regard, *daf-22(ok693)*, as well as *dhs-28(tm2581)*, may be used as a novel nematode model for the human disease Zellweger Syndrome in which a single enzyme (D-BP or SCPx) involved in peroxisomal  $\beta$ -oxidation in humans results in abnormal symptoms such as neonatal hypotonia, craniofacial dysmorphism, seizures and developmental delay [48–51].

In conclusion, our data support a notion that *C. elegans* daumone biosynthesis through peroxisomal  $\beta$ -oxidation seems to have a dual function: detoxification and pheromone production as toxic waste (Figure 7A). In this regard, daumone biosynthesis seems a fundamental part of *C. elegans* homeostasis, affecting both survival and maintenance of physiological well-being. It would be quite useful to explore what would be the key regulatory signal in co-ordinating these two functions under different physiological conditions. Nevertheless, transcriptional control of these two peroxisomal enzymes, DHS-28 and DAF-22, would be an imminent task to understand how these genes are regulated in response to environmental stimulus. Finally, the complete pathway of daumone biosynthesis (Figure 7B) deserves more studies in the context of human disease of peroxisomal metabolism.

Note that during the preparation of the present manuscript, a separate paper appeared on dauer pheromone biosynthesis [23].

## AUTHOR CONTRIBUTIONS

Young-Ki Paik conceived and designed the overall experiments and wrote the manuscript. Hoye-Jin Joo designed the experiments and executed the major parts of this work. Yong-Hyeon Yim and You-Xun Jin performed the GC-MS and LC-MS/MS analyses of fatty acids and their acyl-CoAs. Pan-Young Jeong helped with the initial experiments and Jeong-Eui Lee helped with daumone preparation, qRT-PCR and various phenotype studies. Heekyeong Kim synthesized daumone 1, 2 and 3 and Seul-Ki Jeong performed bioinformatics studies. David Chitwood contributed to a comprehensive interpretation of the results and data analyses.

## ACKNOWLEDGEMENTS

We thank Dr Shohei Mitani (Department of Physiology, Tokyo Women's Medical University, Tokyo, Japan) and the *Caenorhabditis* Genetics Center for provision of all mutants used for this study, Professor Monica Driscoll (Department of Molecular Biology and Biochemistry, Nelson Biological Labs, Piscataway, NJ, U.S.A.) for the gift of  $P_{HSP16.2}$ GFP-SKL construct and Professor Andy Fire for the RNAi vectors. We also thank NBRP (NIG, Japan) for the supply of *E. coli* for JW2686 and JW5435 *E. coli* mutant and Tae Hoon Lee (Yonsei University) for technical help.

## FUNDING

This study was supported by a grant from the Korea Health 21 R&D project, Ministry of Health and Welfare of Republic of Korea [grant number A030003 (to Y.-K. P.)] and a Forest Science & Technology Project through the Korea Forest Service [grant number S110707L0501501 (to Y.-K. P.)].

## REFERENCES

- Golden, J. W. and Riddle, D. L. (1982) A pheromone influences larval development in the nematode *Caenorhabditis elegans*. *Science* **218**, 578–580
- Jeong, P. Y., Jung, M., Yim, Y. H., Kim, H., Park, M., Hong, E., Lee, W., Kim, Y. H., Kim, K. and Paik, Y. K. (2005) Chemical structure and biological activity of the *Caenorhabditis elegans* dauer-inducing pheromone. *Nature* **433**, 541–545
- Riddle, D. L. and Albert, P. S. (1997) Genetic and environmental regulation of dauer larva development. In *C. elegans II* (Riddle, D. L., Blumenthal, T., Meyer, B. J. and Priess, J. R., eds), pp. 739–768. Cold Spring Harbor Laboratory Press, New York
- Cassada, R. C. and Russell, R. L. (1975) The dauerlarva, a post-embryonic developmental variant of the nematode *Caenorhabditis elegans*. *Dev. Biol.* **46**, 326–342
- Kim, S. and Paik, Y. K. (2008) Developmental and reproductive consequences of prolonged non-aging dauer in *Caenorhabditis elegans*. *Biochem. Biophys. Res. Commun.* **368**, 588–592
- Klass, M. and Hirsh, D. (1976) Non-ageing developmental variant of *Caenorhabditis elegans*. *Nature* **260**, 523–525
- Bargmann, C. I. and Horvitz, H. R. (1991) Control of larval development by chemosensory neurons in *Caenorhabditis elegans*. *Science* **251**, 1243–1246
- Zwaal, R. R., Mendel, J. E., Sternberg, P. W. and Plasterk, R. H. (1997) Two neuronal G proteins are involved in chemosensation of the *Caenorhabditis elegans* Dauer-inducing pheromone. *Genetics* **145**, 715–727
- Jeong, P. Y., Kwon, M. S., Joo, H. J. and Paik, Y. K. (2009) Molecular time-course and the metabolic basis of entry into dauer in *C. elegans*. *PLoS ONE* **4**, e4162
- Butcher, R. A., Fujita, M., Schroeder, F. C. and Clardy, J. (2007) Small-molecule pheromones that control dauer development in *Caenorhabditis elegans*. *Nat. Chem. Biol.* **7**, 420–422
- Srinivasan, J., Kaplan, F., Ajredini, R., Zachariah, C., Alborn, H. T., Peter, E. A., Malik, R. U., Edison, A. S., Sternberg, P. W. and Schroeder, F. C. (2008) A blend of small molecules regulates both mating and development in *Caenorhabditis elegans*. *Nature* **28**, 1115–1118
- Butcher, R. A., Ragains, J. R., Kim, E. and Clardy, J. (2008) A potent dauer pheromone component in *Caenorhabditis elegans* that acts synergistically with other components. *Proc. Natl. Acad. Sci. U.S.A.* **105**, 14288–14292
- Batley, J. P. (1996) Structure of the ascariosides from *Ascaris sum.* *J. Nat. Prod.* **59**, 921–926
- Forquy, C., Polonsky, J. and Lederer, E. (1957) Sur la structure chimique de l'alcool ascarylique isolé de *Parascaris equorum*. *Bull. Soc. Chim. Biol.* **39**, 101–132
- Forquy, C., Polonsky, J. and Lederer, E. (1962) Structure chimique des ascariosides A. *Bull. Soc. Chim. Biol.* **44**, 69–81
- Jezyk, P. F. and Fairbairn, D. (1967) Ascariosides and ascarioside esters in *Ascaris lumbricoides* (Nematoda). *Comp. Biochem. Physiol.* **23**, 691–705
- Jezyk, P. F. and Fairbairn, D. (1967) Metabolism of Ascariosides in the ovaries of *Ascaris lumbricoides* (Nematoda). *Comp. Biochem. Physiol.* **23**, 707–719
- He, X. M. and Liu, H. W. (2002) Formation of unusual sugars: mechanistic studies and biosynthetic application. *Annu. Rev. Biochem.* **71**, 701–754
- Matsuhashi, S., Matsuhashi, M., Brown, J. G. and Strominger, J. L. (1964) Enzymatic synthesis of cytidine diphosphate ascarylose. *Biochem. Biophys. Res. Commun.* **15**, 60–64
- Thorson, J. S., Lo, S. F., Ploux, O., He, X. and Liu, H. W. (1994) Studies of the Biosynthesis of 3,6-Dideoxyhexoses: Molecular Cloning and Characterization of the asc (Ascarylose) Region from *Yersinia pseudotuberculosis* Serogroup VA. *J. Bacteriol.* **176**, 5483–5493
- Trefzer, A., Salas, J. A. and Bechthold, A. (1999) Genes and enzymes involved in deoxysugar biosynthesis in bacteria. *Nat. Prod. Rep.* **16**, 283–299
- Golden, J. W. and Riddle, D. L. (1985) A gene affecting production of the *Caenorhabditis elegans* dauer-inducing pheromone. *Mol. Gen. Genet.* **198**, 534–536
- Butcher, R. A., Ragains, J. R., Li, W., Ruvkun, G., Clardy, J. and Mak, H. Y. (2009) Biosynthesis of the *Caenorhabditis elegans* dauer pheromone. *Proc. Natl. Acad. Sci. U.S.A.* **106**, 1875–1879
- Mannaerts, G. P. and van Veldhoven, P. P. (1996) Functions and organization of peroxisomal P-oxidation. *Ann. NY Acad. Sci.* **804**, 99–115
- Brenner, S. (1974) The genetics of *Caenorhabditis elegans*. *Genetics* **77**, 71–94
- Watts, J. L. and Browse, J. (2002) Genetic dissection of polyunsaturated fatty acid synthesis in *Caenorhabditis elegans*. *Proc. Natl. Acad. Sci. U.S.A.* **99**, 5854–5859
- Haynes, C. A., Allegood, J. C., Sims, K., Wang, E. W., Sullards, M. C. and Merrill, A. H. (2008) Quantitation of fatty acyl-coenzyme As in mammalian cells by liquid chromatography-electrospray ionization tandem mass spectrometry. *J. Lipid Res.* **49**, 1113–1125
- Mörck, C. and Pilon, M. (2006) *C. elegans* feeding defective mutants have shorter body lengths and increased autophagy. *BMC Dev. Biol.* **6**, 39–50
- Wong, A., Boutis, P. and Hekimi, S. (1995) Mutations in the *elk-1* gene of *Caenorhabditis elegans* affect developmental and behavioral timing. *Genetics* **139**, 1247–1259
- Oh, S. W., Mukhopadhyay, A., Dixit, B. L., Raha, T., Green, M. R. and Tissenbaum, H. A. (2006) Identification of direct DAF-16 targets controlling longevity, metabolism and diapause by chromatin immunoprecipitation. *Nat. Genet.* **38**, 251–257
- Kimura, K. D., Tissenbaum, H. A., Liu, Y. and Ruvkun, G. (1997) *daf-2*, an insulin receptor-like gene that regulates longevity and diapause in *Caenorhabditis elegans*. *Science* **277**, 942–946
- Mak, H. Y., Nelson, L. S., Basson, M., Johnson, C. D. and Ruvkun, G. (2006) Polygenic control of *Caenorhabditis elegans* fat storage. *Nat. Genet.* **38**, 363–368
- Thieringer, H., Moellers, B., Dodt, G., Kunau, W. H. and Driscoll, M. (2003) Modeling human peroxisome biogenesis disorders in the nematode *C. elegans*. *J. Cell Sci.* **116**, 1797–1804

- 34 Petriv, O., Pilgrim, D. B., Rachubinski, R. A. and Titorenko, V. I. (2002) RNAi interference of peroxisome-related genes in *C. elegans*: a new model for human peroxisomal disorders. *Physiol. Genomics* **10**, 79–91
- 35 Tukey, R. H. and Strassburg, C. P. (200) Human UDP-glucuronosyltransferases: metabolism, expression, and disease. *Annu. Rev. Pharmacol. Toxicol.* **40**, 581–616
- 36 Lindblom, T. H. and Dodd, A. K. (2006) Xenobiotic detoxification in the nematode *Caenorhabditis elegans*. *J. Exp. Zool. A Comp. Exp. Biol.* **305**, 720–730
- 37 Lewis, J. A., Szilagyi, M., Gehman, E., Dennis, W. E. and Jackson, D. A. (2009) Distinct patterns of gene and protein expression elicited by organophosphorus pesticides in *Caenorhabditis elegans*. *BMC Genomics* **10**, 202
- 38 Russell, D. W. (2003) The enzymes, regulation and genetics of bile acid biosynthesis. *Annu. Rev. Biochem.* **72**, 137–174
- 39 Ferdinandusse, S., Denis, S., Dacremont, G. and Wanders, R. J. (2009) Toxicity of peroxisomal C27-bile acid intermediates. *Mol. Genet. Metab.* **96**, 121–128
- 40 Gallo, M. and Riddle, D. L. (2009) Effects of a *Caenorhabditis elegans* dauer pheromone ascaroside on physiology and signal transduction pathways. *J. Chem. Ecol.* **35**, 272–279
- 41 Tarr, G. E. and Schones, H. K. (1973) Structures of ascaroside aglycones. *Arch. Biochem. Biophys.* **158**, 288–296
- 42 Beames, C. G., Harris, B. G. and Hopper, F. A. (1967) The synthesis of fatty acids from acetate by intact tissue and muscle extract of *Ascaris lumbricoide* ssum. *Comp. Biochem. Physiol.* **20**, 509–521
- 43 Visser, W. F., van Roermund, C. W., Ijlst, L., Waterham, H. R. and Wanders, R. J. (2007) Metabolite transport across the peroxisomal membrane. *Biochem. J.* **401**, 365–375
- 44 Hunt, M. C. and Alexson, S. E. (2008) Novel functions of acyl-CoA thioesterases and acyltransferases as auxiliary enzymes in peroxisomal lipid metabolism. *Prog. Lipid Res.* **47**, 405–421
- 45 Oey, N. A., Ijlst, L., van Roermund, C. W., Wijburg, F. A. and Wanders, R. J. (2005) dif-1 and colt, both implicated in early embryonic development, encode carnitine acylcarnitine translocase. *Mol. Genet. Metab.* **85**, 121–124
- 46 Verhoeven, N. M., Roe, D. S., Kok, R. M., Wanders, R. J., Jakobs, C. and Roe, C. R. (1998) Phytanic acid and pristanic acid are oxidized by sequential peroxisomal and mitochondrial reactions in cultured fibroblasts. *J. Lipid Res.* **39**, 66–74
- 47 Verhoeven, N. M. and Jakobs, C. (2001) Human metabolism of phytanic acid and pristanic acid. *Prog. Lipid Res.* **40**, 453–466
- 48 Brites, P., Moyer, P. A. W., Mrabet, L., Waterham, H. R. and Wanders, R. J. A. (2009) Plasmalogen participate in very long chain fatty acid induced pathology. *Brain* **132**, 482–492
- 49 Wanders, R. J. and Waterham, H. R. (2006) Peroxisomal disorders: the single peroxisomal enzyme deficiencies. *Biochim. Biophys. Acta.* **1763**, 1707–1720
- 50 Clayton, P. T. (2001) Clinical consequences of defects in peroxisomal  $\beta$ -oxidation. *Biochem. Soc. Trans.* **29**, 298–305
- 51 Wanders, R. J. (2004) Peroxisomes, lipid metabolism, and peroxisomal disorders. *Mol. Genet. Metab.* **83**, 16–27

Received 31 March 2009/3 June 2009; accepted 4 June 2009

Published as BJ Immediate Publication 4 June 2009, doi:10.1042/BJ20090513

**SUPPLEMENTARY ONLINE DATA**

***Caenorhabditis elegans* utilizes dauer pheromone biosynthesis to dispose of toxic peroxisomal fatty acids for cellular homeostasis**

Hyoe-Jin JOO\*, Yong-Hyeon YIM†, Pan-Young JEONG\*<sup>1</sup>, You-Xun JIN†, Jeong-Eui LEE\*, Heekyeong KIM\*<sup>2</sup>, Seul-Ki JEONG\*, David J. CHITWOOD‡ and Young-Ki PAIK\*<sup>3</sup>

\*Department of Biochemistry, College of Life Sciences and Biotechnology, Yonsei Proteome Research Center, Yonsei University, Seoul 120-749, Republic of Korea,

†Korea Research Institute of Standards and Science, Daejeon 305-340, Republic of Korea, and ‡Nematology Laboratory, USDA, ARS, Beltsville, MD 20705, U.S.A.

**Table S1** Compositions of major buffers used in experiments in the present study

Name	Composition
Lysis buffer	200 mM Tris/HCl, pH 8.0, 500 mM NaCl, 0.1 mM EDTA, 0.1% Triton X-100 and 0.4 mM PMSF
S-basal buffer	5 g NaCl and 50 ml of 1 M potassium phosphate per litre
M9 buffer	6 g Na <sub>2</sub> HPO <sub>4</sub> , 3 g KH <sub>2</sub> PO <sub>4</sub> , 5 g NaCl and 0.25 g MgSO <sub>4</sub> ·7H <sub>2</sub> O per litre
Blocking buffer	5% (w/v) non-fat dried skimmed milk powder and 0.05% (w/v) sodium azide in TBST (TBST: 150 mM NaCl, 50 mM Tris/HCl, pH 8.0, and 0.1% Tween 20)

**Table S2** LC gradient elution conditions for the separation of daumones

Eluent A: 10 mM ammonium formate and 0.1% formic acid; eluent B: acetonitrile and 0.1% formic acid

Gradient	
Time (min)	B (%)
0.0	8
12.0	95
19.0	95
19.1	8

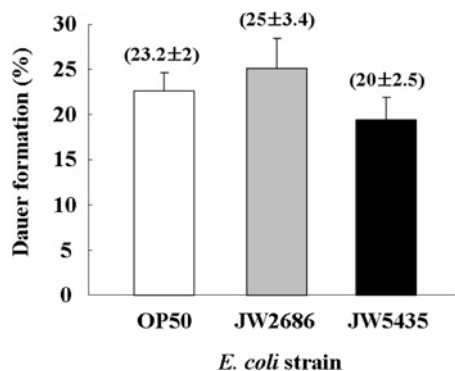


**Figure S1** Origin of ascaylose in daumone biosynthesis

Dauer formation rate was measured by liquid culture assay using N2 worms that had been grown in K-12 *E. coli* mutants (*ascB*[del]:JW2686 and *ascF*[del]:JW5435) lacking the ascarylose synthesis gene. After 10 days of culture, dauer formation was measured (means ± S.D., *n* > 1500) as a percentage of the total population. The results represent data from two independent experiments.

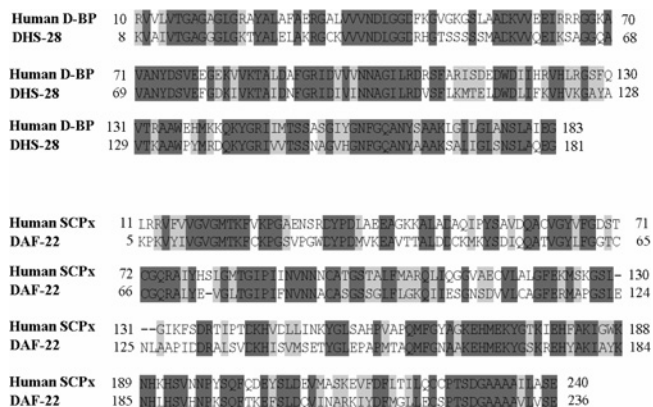


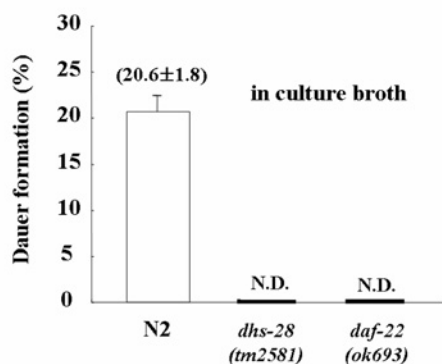
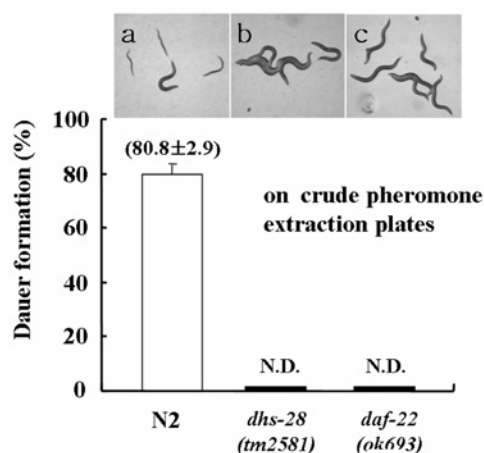
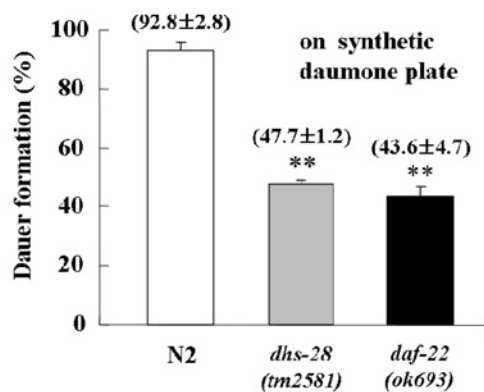
**Figure S2** Alignment of amino acid sequence homologies between human D-BP and *C. elegans* DHS-28 and human SCPx and *C. elegans* DAF-22

Upper panel: amino acid sequence alignment of the SDR (short chain dehydrogenase and hydratase) domain between human D-BP (10–183 aa/total 736 aa) and DHS-28 (8–181 aa/total 436 aa). Bottom panel: amino acid sequence alignment of the thiolase domain between human SCPx (11–240 aa/total 547 aa) and DAF-22 (5–236 aa/total 412 aa). This was performed by screening *C. elegans* homologous genes corresponding to the enzymes involved in the predicted peroxisomal β-oxidation [reactions (ii)–(iv) in Figure 1B] through NCBI (<http://www.ncbi.nlm.nih.gov>) and PSORT II databases (<http://psort.ims.u-tokyo.ac.jp/>).

<sup>1</sup> Present address: Department of Molecular, Cellular and Developmental Biology, University of California Santa Barbara, Santa Barbara, CA 93106, U.S.A.

<sup>2</sup> Present address: Graduate Program in Biomaterials, Science and Engineering, Yonsei University, Seoul 120-749, Republic of Korea.

<sup>3</sup> To whom correspondence should be addressed (email paiky@yonsei.ac.kr).

**A****B****C**

**Figure S3** *dhs-28(tm2581)* and *daf-22(ok693)* are defective in dauer pheromone biosynthesis

(A) Dauer formation rate in wild-type N2, *dhs-28(tm2581)* and *daf-22(ok693)* mutants in liquid culture. Worms were grown in liquid broth at 20°C for 10 days, during which fresh food in the form of fresh *E. coli* had been supplied at day 4 or 5 to induce a high population density

**Table S3** Mass spectrometer settings for selected quantification of fatty acyl-CoAs

Fatty acyl-CoA	Precursor ion ( <i>m/z</i> )	Product ion ( <i>m/z</i> )	Collision energy (% full excitation)
14:0	976.4	629.3	17
15:0	990.4	643.3	17
16:0	1004.4	657.3	17
17:0	1018.4	671.3	17
18:0	1032.4	685.3	17
aOH-18:0	1048.4	701.3	17
18:1	1030.4	683.3	17
18:2	1028.4	681.3	17
18:3	1026.4	679.3	17
20:0	1060.4	713.3	20
20:4	1052.4	705.3	20
22:0	1088.4	741.3	20
22:6	1076.4	729.3	20
23:0	1102.4	755.3	20
24:0	1116.4	769.3	20
24:1	1114.4	767.3	20
25:0	1130.4	783.3	20
26:0	1144.4	797.3	20
15:1	988.4	641.3	17
17:1	1016.4	669.3	17
19:0	1046.4	699.3	20
19:1	1044.4	697.3	20
21:0	1074.4	727.3	20
21:1	1072.4	725.3	20
13:0	962.4	615.3	17
13:1	960.4	613.3	17
12:0	948.4	601.3	17
11:0	934.4	587.3	17
11:1	932.4	585.3	17
10:0	920.4	573.3	17
9:0	906.4	559.3	17
9:1	904.4	557.3	17
8:0	892.4	545.3	17
7:0	878.4	531.3	17
7:1	876.4	529.3	17
6:0	864.4	517.3	17

(> 50000 worms/ml). Results are from at least three independent experiments, means ± SD,  $n > 1500$ ; N.D., not detected. (B) Dauer formation rate of N2 in the presence of 20 mg crude dauer pheromone extracts obtained from the culture broth of N2, *dhs-28(tm2581)* and *daf-22(ok693)*. Upper panels depict morphological patterns of each strain. Each experiment was performed in triplicate, and results are means ± S.D.  $n > 150$ ; N.D., not detected. (C) Dauer formation rate of N2, *dhs-28(tm2581)* and *daf-22(ok693)* on the dauer pheromone plates. Dauer assay was carried out as described in [1]. Each experiment was performed in triplicate, and results are means ± S.D.,  $n > 150$ . \*\* $P < 0.0001$  compared with N2.  $P$  values were derived from  $t$  test.

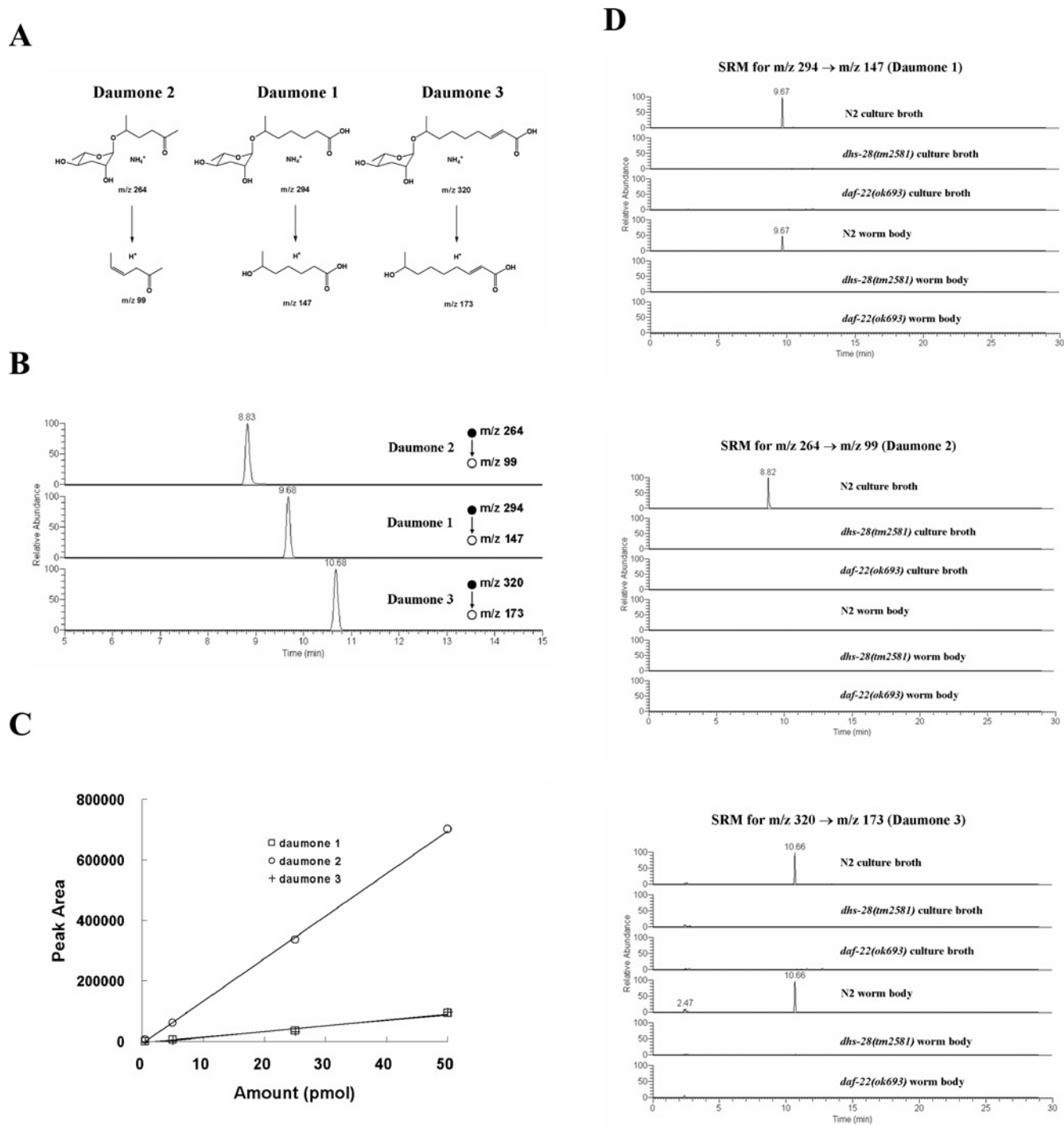


**Figure S4 Quantitative analysis of daumones 1, 2 and 3 in N2, *dhs-28(tm2581)* and *daf-22(ok693)***

(A) Fragmentation reactions used for selected reaction monitoring. (B) LC-ESI MS/MS chromatograms of 50 pmol daumone standards. (C) Relationships between peak area and amount of daumones injected for LC-MS/MS analysis. (D) LC-MS/MS analysis of daumones 1, 2 and 3 in culture broth and worm body for N2, *dhs-28* and *daf-22* mutants. All chromatograms are normalized to the same scale. The flow rate of the mobile phase (gradient described in Table S1) was 0.2 ml/min. For selective and reliable quantification of daumone species, SRM was used. Fragmentations of  $(M + \text{NH}_4)^+$  precursor ions of daumones into selective product ions resulting from concomitant loss of ammonia and ascaryleose unit were used as SRM channels.

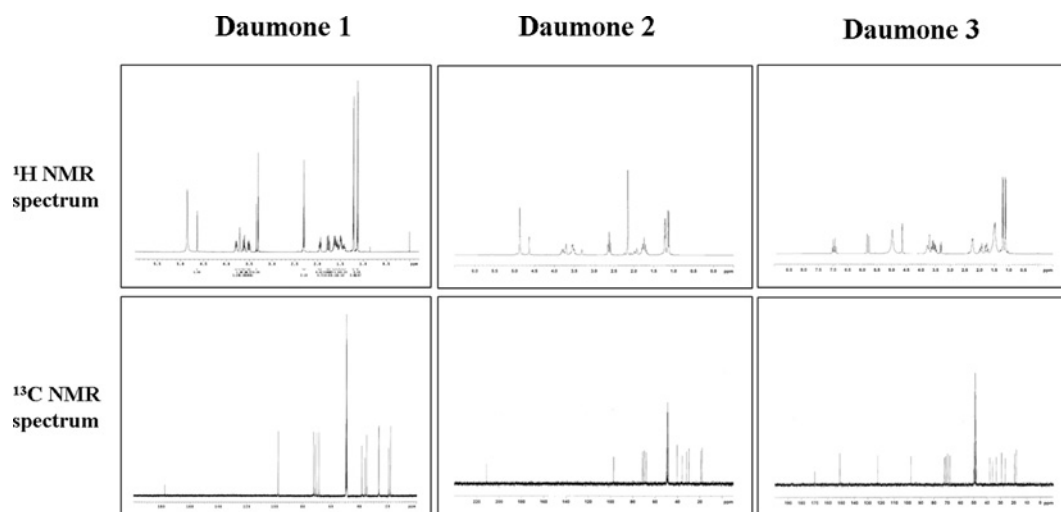


**Figure S5** NMR spectra of synthetic daumones 1, 2 and 3

NMR spectra of synthetic daumones 1, 2 and 3 in methanol- $d_4$ . Our NMR data on daumone synthesis are consistent with published studies [2–4]. Top panels,  $^1\text{H}$  NMR spectrum of synthetic daumones 1, 2 and 3 in methanol- $d_4$ . Bottom panels,  $^{13}\text{C}$  NMR spectrum of synthetic daumones 1, 2 and 3 in methanol- $d_4$ .

**Table S4** Developmental growth rate of N2, *dhs-28(tm2581)* and *daf-22(ok693)*

Developmental time from egg: 72 h. The numbers in each column represent means  $\pm$  S.D. (from triplicate sets.). \*\* $P < 0.0001$  compared with N2 (L4 stage).  $P$  values were derived from the  $t$  test.

Developmental stage	N2	<i>daf-22(ok693)</i>	<i>dhs-28(tm2581)</i>	<i>daf-22(ok693);</i> <i>dhs-28(tm2581)</i>
L1	0	0	0	0
L2	0	0	$0.4 \pm 0.7$	$2.7 \pm 1.2$
L3	$1.1 \pm 1.0$	$8.0 \pm 1.4$	$5.4 \pm 0.7$	$9.2 \pm 2.9$
L4	$5.1 \pm 3.0$	$86.0 \pm 4.0^{**}$	$94.1 \pm 0.6^{**}$	$88 \pm 3.3^{**}$
Adult	$93.8 \pm 2.2$	$6.1 \pm 4.6$	0	0

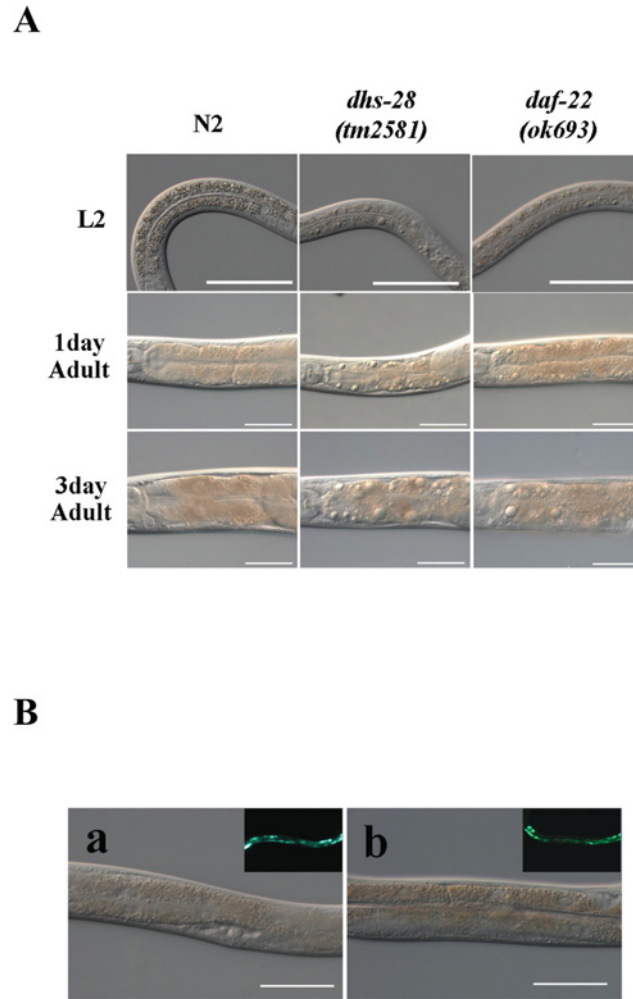


**Figure S6 Fat granule phenotype in the intestines of *C. elegans* N2, *dhs-28(tm2581)* and *daf-22(ok693)***

(A) The fat granules of *dhs-28(tm2581)* and *daf-22(ok693)* increase as development proceeds. The intestines of N2, *dhs-28(tm2581)* and *daf-22(ok693)* at L2, 1 day and 3 day adult stage were observed by Nomarski microscopy. Bar = 50  $\mu$ m. (B) Rescue of the fat granule phenotype in *dhs-28(tm2581)* and *daf-22(ok693)*. (a) The intestine of the injected *dhs-28(tm2581)* worm with *dhs-28* full gene-containing GFP vector (*dhs-28 Prom::GFP::dhs-28* full gene). We observed that fat granules in the *dhs-28(tm2581)* were reduced or disappeared in the intestine. (b) The intestine of the injected *daf-22(ok693)* worm with *daf-22* full gene-containing GFP vector (*daf-22 Prom::GFP::daf-22* full gene). The fat granule in injected *daf-22(ok693)* worms was reduced or disappeared, similar to *dhs-28* rescue worms. The small box in (a) and (b) shows the expression of each rescue GFP vector. The worm is L4 stage. Bar = 50  $\mu$ m.

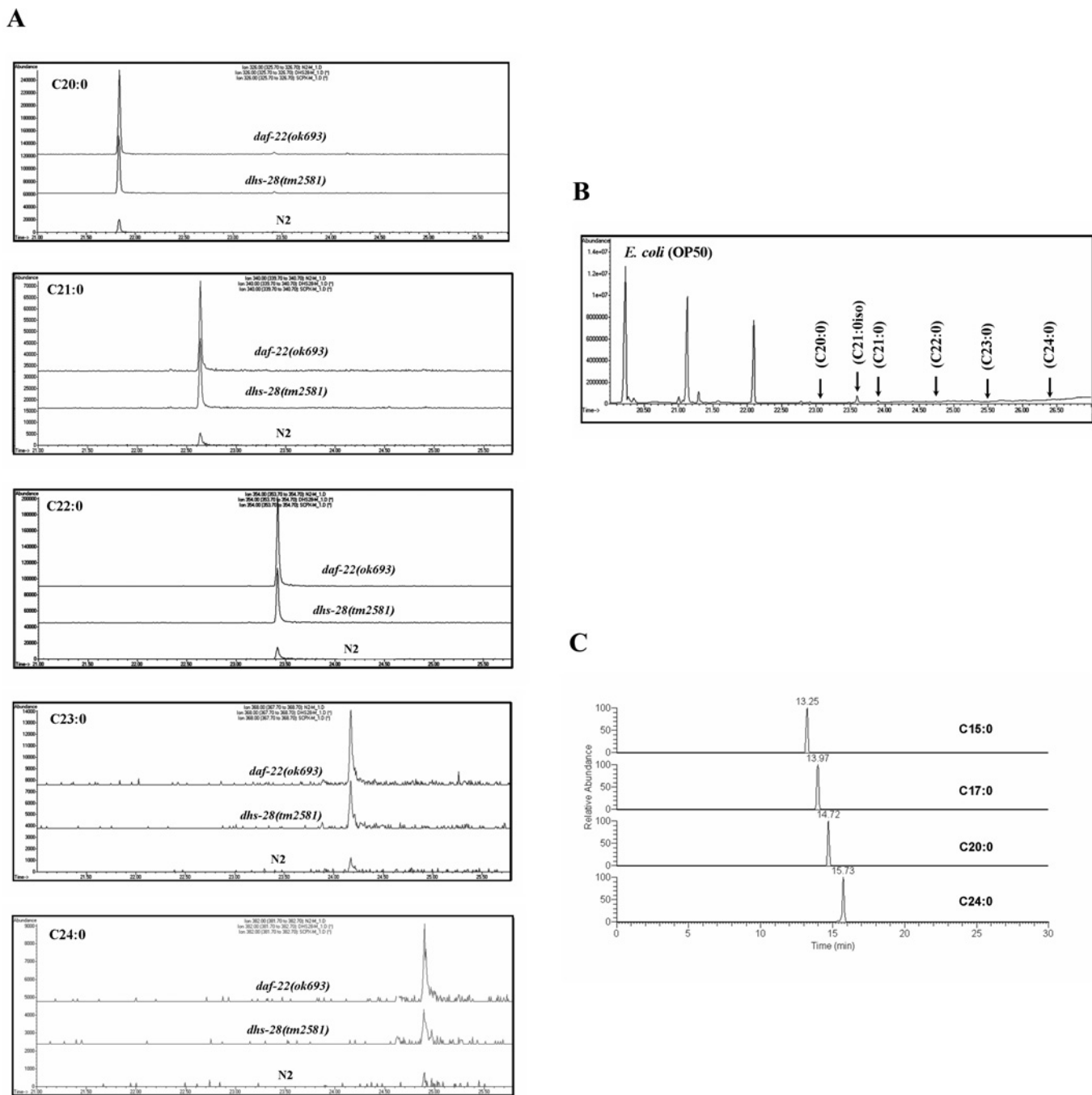


**Figure S7 GC-MS and LC-MS/MS analysis of fatty acid and fatty acyl-CoA**

(A) Selected ion chromatograms from GC-MS analysis of fatty acid methyl esters in N2, *dhs-28* and *daf-22* worms. Approx. 1.0 ml of 2.5% methanolic H<sub>2</sub>SO<sub>4</sub> was then added, and the worm samples were heated for 1 h at 90 °C. After cooling the samples, 1.0 ml of hexane and 1.5 ml of H<sub>2</sub>O were added and mixed thoroughly. Methyl esters of fatty acids were extracted into the hexane layer (upper phase) by shaking and centrifuging at low speed. Only chromatograms for long-chain fatty acids, which show significant change in the relative abundance in the mutants, are presented here; C20:0 (*m/z* 326), C21:0 (*m/z* 340), C22:0 (*m/z* 354), C23:0 (*m/z* 368), C24:0 (*m/z* 382). (B) GC chromatogram of fatty acid distribution in *E. coli* (OP50). (C) LC-ESI MS/MS chromatograms of 10 pmol of fatty acyl-CoA standards.

## REFERENCES

- 1 Cassada, R. C. and Russell, R. L. (1975) The dauerlarva, a post-embryonic developmental variant of the nematode *Caenorhabditis elegans*. *Dev. Biol.* **46**, 326–342
- 2 Butcher, R. A., Fujita, M., Schroeder, F. C. and Clardy, J. (2007) Small-molecule pheromones that control dauer development in *Caenorhabditis elegans*. *Nat. Chem. Biol.* **7**, 420–422
- 3 Srinivasan, J., Kaplan, F., Ajredini, R., Zachariah, C., Alborn, H. T., Peter, E. A., Malik, R. U., Edison, A. S., Sternberg, P. W. and Schroeder, F. C. (2008) A blend of small molecules regulates both mating and development in *Caenorhabditis elegans*. *Nature* **28**, 1115–1118
- 4 Butcher, R. A., Ragains, J. R., Kim, E. and Clardy, J. (2008) A potent dauer pheromone component in *Caenorhabditis elegans* that acts synergistically with other components. *Proc. Natl. Acad. Sci. U.S.A.* **105**, 14288–14292

---

Received 31 March 2009/3 June 2009; accepted 4 June 2009

Published as BJ Immediate Publication 4 June 2009, doi:10.1042/BJ20090513